

## Removal of Gas-Phase Element Mercury by Activated Carbon Fiber Impregnated with CeO<sub>2</sub>

Xiaopeng Fan,<sup>†,‡</sup> Caiting Li,<sup>\*,†,‡</sup> Guangming Zeng,<sup>†,‡</sup> Zhao Gao,<sup>†,‡</sup> Ling Chen,<sup>†,‡</sup> Wei Zhang,<sup>†,‡</sup> and Hongliang Gao<sup>†,‡</sup>

<sup>†</sup>College of Environmental Science and Engineering, Hunan University, Changsha 410082, People's Republic of China, and  
<sup>‡</sup>Key Laboratory of Environmental Biology and Pollution Control, Hunan University, Ministry of Education, Changsha 410082, People's Republic of China

Received March 28, 2010. Revised Manuscript Received July 2, 2010

The Hg<sup>0</sup> removal ability of activated carbon fiber (ACF) impregnated with cerium dioxide (CeO<sub>2</sub>/ACF) was tested in experimental gas. Some physicochemical techniques, such as Brunauer–Emmett–Teller (BET), scanning electron microscopy (SEM), and Fourier transform infrared (FTIR) spectroscopy, were used to characterize the samples. The effects of loading values, calcination temperatures, reaction temperatures, and acid gases, such as NO and SO<sub>2</sub>, on the Hg<sup>0</sup> removal rates were investigated. The experimental results showed that impregnation with CeO<sub>2</sub> significantly enhanced the Hg<sup>0</sup> removal ability of ACF, particularly with the loading value of 6%. The samples at different calcination temperatures had a similar Hg<sup>0</sup> removal performance. When the temperature was below 150 °C, the CeO<sub>2</sub>/ACF removal ability for Hg<sup>0</sup> was enhanced with the increase of the temperature and then decreased after 150 °C. NO and SO<sub>2</sub> of the experimental gas were found to have a promoted effect on Hg<sup>0</sup> oxidation.

### 1. Introduction

Mercury cycling in the environment is important on a global scale, because mercury can be released into the atmosphere and bioaccumulate in the food chain, causing adverse effects on human health and the environment.<sup>1–4</sup> Mercury often exists in trace amounts in coal. Because of the large quantity of coal burning, the emission of mercury from coal-fired utilities has become the main anthropogenic mercury pollution source for countries using coal as their principal energy input.<sup>5–7</sup> Thus, development of technologies governing/controlling Hg emission from coal-fired power plants is an urgent issue.

Mercury in coal-fired flue gas is often present as elemental mercury vapor (Hg<sup>0</sup>), oxidized mercury vapor (Hg<sup>2+</sup>), and particle-bound mercury (Hg<sup>p</sup>).<sup>8</sup> Different species of mercury have different physical and chemical properties. Hg<sup>p</sup> can be easily collected by dust removal devices from the flue gas. Hg<sup>2+</sup> is soluble in water and has the tendency to associate with particulate matter. Thus, air pollution control devices, such as an electrostatic precipitator (ESP) and wet flue gas desulfurization (WFGD), can remove Hg<sup>2+</sup>. However, all of these

devices are ineffective in capturing Hg<sup>0</sup> because of its low melting point (–38.9 °C), high equilibrium vapor pressure (0.25 Pa at 25 °C), and low solubility in water (60 mg/m<sup>3</sup> at 25 °C),<sup>9</sup> therefore, most elemental mercury is released into the atmosphere. With consideration of the properties of Hg<sup>2+</sup>, Hg<sup>p</sup>, and Hg<sup>0</sup>, development of an efficient method for the removal of Hg<sup>0</sup> should be taken into account at first.

A lot of current research on the approaches of removing Hg<sup>0</sup> from the fuel gas focuses on sorbent injection and Hg<sup>0</sup> oxidation methods. Activated carbon injection technology is a kind of Hg<sup>0</sup>-removing approach frequently adopted, especially chemically treated activated carbon with elements such as sulfur, chlorine, or iodine.<sup>9–11</sup> However, remarkable disadvantages using activated carbon for Hg<sup>0</sup> removal can be found in higher operation expenses, poor capacity, and deteriorated fly ash.<sup>12,13</sup> Therefore, the development of Hg<sup>0</sup> oxidation methods attracts more and more attention. It has been reported that activated carbon impregnated with some metal oxides (CuO, V<sub>2</sub>O<sub>5</sub>, Cr<sub>2</sub>O<sub>3</sub>, MnO<sub>2</sub>, Fe<sub>2</sub>O<sub>3</sub>, etc.) is effective for Hg<sup>0</sup> removal.<sup>14–18</sup> However, cerium dioxide

\*To whom correspondence should be addressed. Telephone: +86-731-88649216. E-mail: cttli3@yahoo.com.

(1) Lindberg, S. E.; Stratton, W. J. *Environ. Sci. Technol.* **1998**, *32*, 49–57.

(2) Brown, T. D.; Smith, D. N.; Hargis, R. A. *J. Air Waste Manage. Assoc.* **1999**, *49*, 628–640.

(3) Mei, Z. J.; Shen, Z. M.; Yuan, T.; Wang, W. H.; Han, H. B. *Fuel Process. Technol.* **2007**, *88*, 623–629.

(4) Dastoor, A. P.; Larocque, Y. *Atmos. Environ.* **2004**, *38*, 147–161.

(5) Ebinghaus, R.; Kock, H. H.; Temme, C. *Environ. Sci. Technol.* **2002**, *36*, 1238–1244.

(6) Wang, Q. C.; Shen, W. G.; Ma, Z. W. *Environ. Sci. Technol.* **2000**, *34*, 2711–2713.

(7) Wu, Y.; Wang, S. X.; Streets, D. G. *Environ. Sci. Technol.* **2006**, *40*, 5312–5318.

(8) Guo, S. Q.; Yang, J. L.; Liu, Z. Y. *Energy Fuels* **2009**, *23*, 4817–4821.

(9) Zeng, H. C.; Jin, F.; Guo, J. *Fuel* **2004**, *83*, 143–146.

(10) Vidic, R. D.; Siler, D. P. *Carbon* **2001**, *39*, 3–14.

(11) Ghorishi, S. B.; Robert, M. K.; Shannon, D. S.; Brian, K. G.; Wojciech, S. J. *Environ. Sci. Technol.* **2002**, *36*, 4454–4459.

(12) Granite, E. J.; Freeman, M. C.; Hargis, R. A.; O'Dowd, W. J.; Pennline, H. W. *J. Environ. Manage.* **2007**, *84*, 628–634.

(13) Bolger, P. T.; Szlag, D. C. *Environ. Sci. Technol.* **2002**, *36*, 4430–4435.

(14) Poulston, S.; Granite, E. J.; Pennline, H. W.; Myers, C. R.; Stanko, D. P. *Fuel* **2007**, *86*, 2201–2203.

(15) Li, J. F.; Yan, N. Q.; Qu, Z.; Qiao, S. H.; Yang, S. J.; Guo, Y. F.; Liu, P.; Jia, J. P. *Environ. Sci. Technol.* **2010**, *44*, 426–431.

(16) Pitoniak, E.; Wu, C. Y.; Mazyck, D. W. *Environ. Sci. Technol.* **2005**, *39*, 1269–1274.

(17) Ji, L.; Sreekanth, P. M.; Smirniotis, P. G. *Energy Fuels* **2008**, *22*, 2299–2306.

(18) Straube, S.; Hahn, T.; Koester, H. *Appl. Catal., B* **2008**, *79*, 286–295.

(CeO<sub>2</sub>) used as an efficient promoter in chemical processes was rarely reported in the Hg<sup>0</sup> removal procedure. Meanwhile, activated carbon fiber (ACF) has certain advantages, including very fast adsorption rates, a larger adsorption capacity, less attrition, channel, and bypass flows arising from packing the granular carbon system, and high efficiency for the absorption of NO, SO<sub>2</sub>, VOCs, etc.<sup>19–22</sup> In this work, ACF impregnated with CeO<sub>2</sub> (CeO<sub>2</sub>/ACF) was developed and evaluated in a lab-scale fixed-bed system to produce an effective mercury sorbent for coal-fired power plants.

## 2. Experimental Section

**2.1. Sample Preparation.** The commercially available ACF (Jiangsu Sutong Carbon Fiber Company) was ground and washed with deionized water and then dried in an electric blast drying oven at 90 °C for 24 h. Then, the sample was stored in a desiccator for future use.

ACF impregnated with CeO<sub>2</sub> was prepared by the thermal decomposition of Ce(NO<sub>3</sub>)<sub>3</sub>·6H<sub>2</sub>O loaded on ACF as follows: Ce(NO<sub>3</sub>)<sub>3</sub>·6H<sub>2</sub>O was dissolved in deionized water to form the solution. Then, the ACF was added into the solution with stirring in a proportion corresponding to different loading values ( $\rho$ , which is the mass ratio of CeO<sub>2</sub>/ACF) varied from 2 to 15 wt %. In this serial experiment, a solution/ACF ratio of 4 mL/g was used. The samples were dried in an electric blast drying oven at 90 °C for 24 h. Finally, the decomposition of the cerium precursor yielding CeO<sub>2</sub>/ACF was accomplished under a N<sub>2</sub> atmosphere at 300, 400, and 500 °C for 3 h. Then, CeO<sub>2</sub>/ACF was cooled to room temperature and stored in a desiccator.

**2.2. Sample Characterization.** Textural characteristics of samples were explored by nitrogen adsorption at –196 °C on a Micromeritics ASAP 2010 analyzer. The specific surface area was calculated on the basis of the Brunauer–Emmett–Teller (BET) method. The pore size distribution was characterized using the desorption branches of the N<sub>2</sub> adsorption isotherm and the Barrett–Joyner–Halenda (BJH) formula. All of the sorbents were degassed at 120 °C prior to BET measurements.

To further investigate the removal ability of mercury, micrographs of the sample surface were obtained by means of JSM-6700F after vacuum plating Au film.

Fourier transform infrared (FTIR) spectroscopy was recorded on a WQF-410 FTIR spectrometer with a deuterated triglycine sulfate (DTGS) detector. In the experiment, the FTIR spectra were recorded by accumulating 32 scans at a spectra resolution of 4 cm<sup>–1</sup>.

The Hg concentrations in the vapor phase were analyzed by employing a QM201G portable mercury analyzer purchased from the Suzhou Greencalm Instruments Company, Limited. In the Hg<sup>0</sup> analyzer, the sample gas was first dehumidified by silica gel and then put into the mercury collector, in which Hg<sup>0</sup> was collected by the gold membrane. After collection, the gold membrane was heated to the desired temperature to release Hg<sup>0</sup>, which was measured via cold-vapor atomic fluorescence spectroscopy, whose detection limit is 0.001 μg/m<sup>3</sup>, with a nominal range of 0.01–100 μg/m<sup>3</sup>.

**2.3. Adsorption Test.** A schematic diagram of the experimental setup is shown in Figure 1. The apparatus consisted of an experimental gas system, a fixed-bed reactor, and a Hg<sup>0</sup> analyzer. The experimental gas consisted of five major components: O<sub>2</sub>, N<sub>2</sub>, NO, CO<sub>2</sub>, and SO<sub>2</sub>. The N<sub>2</sub> flow was divided into two branches: one branch converged with NO, CO<sub>2</sub>, O<sub>2</sub>, and SO<sub>2</sub> to form the main gas flow, while the other passed through a Hg<sup>0</sup> permeation tube (VICI Metronics) and introduced the saturated Hg<sup>0</sup> vapor into the system. The Hg<sup>0</sup> permeation tube was placed

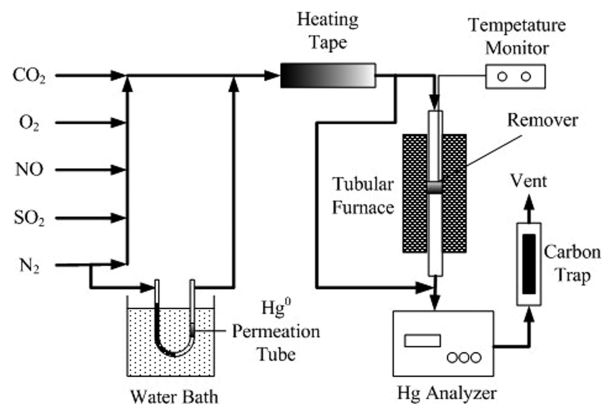


**Figure 1.** Schematic diagram of the experimental setup.

in a U-shape glass tube, which was immersed in a constant temperature water bath to ensure a constant Hg<sup>0</sup> permeation rate. The Hg<sup>0</sup> concentration in the system was controlled at 20.02 μg/m<sup>3</sup>. The gas concentrations were designed to be within the range of a typical coal-fired flue gas composition: 5% O<sub>2</sub>, 10% CO<sub>2</sub>, 800 ppm NO, 1000 ppm SO<sub>2</sub>, and a balance of N<sub>2</sub>. Water, which is a significant component in coal flue gas, was not included in the experimental gas. The total flux was controlled at 1 L/min in each project using a mass flowmeter.

Because quartz has been demonstrated to have good chemical resistance and inertness toward mercury, a quartz tube with an inner diameter of 10 mm held in a vertical position was used as the reactor, which was surrounded by a large tubular furnace, and about 0.1 g of the remover was packed in it. A temperature control device was employed to keep the adsorbent bed at the desired temperature. The inlet and outlet Hg<sup>0</sup> concentrations were measured by the mercury analyzer. After the analysis, the exhaust gas emission from the mercury analyzer was introduced into the activated carbon trap before being expelled into the air.

During the experiment, the experimental gas bypassed the quartz tube and was introduced into the analytical system until the desired inlet mercury concentration had been established for 20 min. Then, the experiment was initiated by diverting the gas flow through the quartz tube. For the whole tests, the Hg<sup>0</sup> removal efficiency ( $\eta$ ) was quantified by a comparison between the Hg<sup>0</sup> concentration of the inlet and the outlet of the quartz tube.  $\eta$  is defined in eq 1 as

$$\eta = \frac{Hg_{inlet}^0 - Hg_{outlet}^0}{Hg_{inlet}^0} \times 100\% \quad (1)$$

## 3. Results and Discussion

**3.1. Sample Characteristics.** Porous structure parameters of the samples are shown in Table 1. It can be seen from the table that ACF has the highest BET surface area value of 1589.5 m<sup>2</sup>/g and total pore volume value of 0.87 cm<sup>3</sup>/g. However, the BET surface area, total pore volume, and pore size of ACF decreased with an increasing concentration of CeO<sub>2</sub>. For example, when ACF was loaded with 15% CeO<sub>2</sub>, the BET surface area was reduced from 1589.5 to 965.3 m<sup>2</sup>/g, the total pore volume was reduced from 0.87 to 0.51 cm<sup>3</sup>/g, and the pore size changed from 1.9 to 1.3 nm because the metal oxide conglomerations were mainly located on the surface of ACF and little in the pores, which could cause destruction of the thin pore walls and blocking of internal porosity.<sup>23–25</sup>

(19) Das, D.; Gaur, V.; Verma, N. *Carbon* **2004**, *42*, 2949–2962.

(20) Lu, A. H.; Zheng, J. T. *Carbon* **2002**, *40*, 1353–1361.

(21) Gaur, V.; Asthana, R.; Verma, N. *Carbon* **2006**, *44*, 46–60.

(22) Mochida, I.; Korai, Y.; Shirahama, M. *Carbon* **2000**, *38*, 227–239.

(23) Kuang, M.; Yang, G. H.; Chen, W. J.; Zhang, Z. X. *J. Fuel Chem. Technol.* **2008**, *36*, 468–473.

(24) Lu, P.; Li, C. T.; Zeng, G. M.; He, L. J.; Peng, D. L.; Cui, H. F.; Li, S. H.; Zhai, Y. B. *Appl. Catal., B* **2010**, *96*, 157–161.

(25) Li, Y. H.; Lee, C. W.; Gullett, B. K. *Fuel* **2003**, *82*, 451–457.

**Table 1. Porous Structure Parameters of the Samples**

samples	BET surface area (m <sup>2</sup> /g)	total pore volume (cm <sup>3</sup> /g)	pore size (nm)
ACF	1589.5	0.87	1.9
2% CeO <sub>2</sub> /ACF	1345.9	0.72	1.6
6% CeO <sub>2</sub> /ACF	1275.4	0.68	1.5
10% CeO <sub>2</sub> /ACF	1193.3	0.65	1.4
15% CeO <sub>2</sub> /ACF	965.3	0.51	1.3

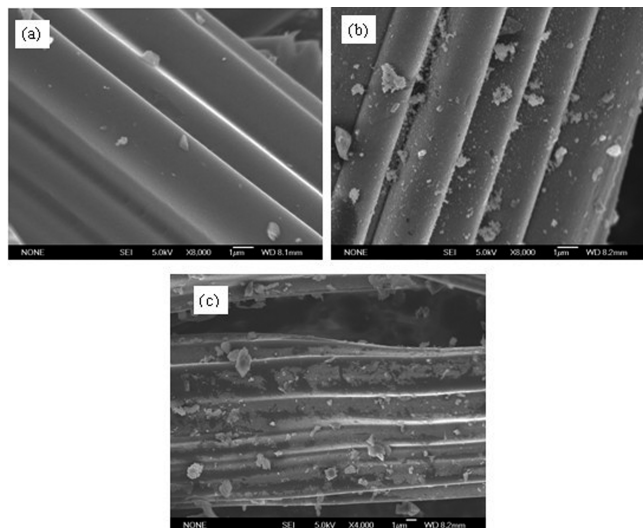
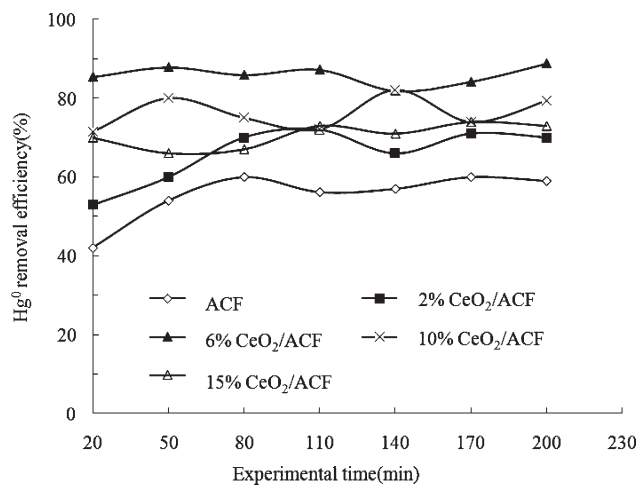
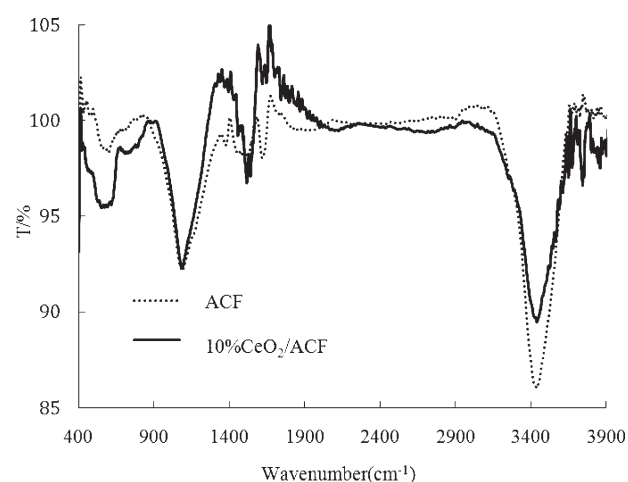
**Figure 2.** SEM photographs of (a) ACF, (b) 6% CeO<sub>2</sub>/ACF, and (c) 6% CeO<sub>2</sub>/ACF after the reaction.

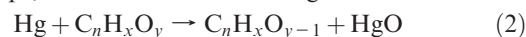
Figure 2 shows the scanning electron microscope (SEM) images of ACF, 6% CeO<sub>2</sub>/ACF, and 6% CeO<sub>2</sub>/ACF after the reaction. Dark zones indicate the presence of carbon fiber, while light zones demonstrate the presence of metal oxides. It can be seen from Figure 2a that the surface of ACF is smooth and the ACF microcrystal line structure is clear, without any particle adsorbed. As shown in Figure 2b, cerium oxide is highly dispersed on the activated carbon fiber surface and only a few cerium oxide agglomerates exist. Furthermore, there are small holes at the surface of 6% CeO<sub>2</sub>/ACF, which indicate that cerium oxide modified the structure of ACF. In comparison to Figure 2b, Figure 2c illustrates that there are more light zones on the surface of 6% CeO<sub>2</sub>/ACF after the reaction. The former agglomerates shown in Figure 2b do not rupture and vanish from the ACF surface, which indicated that a large number of new substances, which could be Hg<sup>0</sup>, were adsorbed on the ACF surface in the reaction.

**3.2. Effects of Loading Values.** The effects of the CeO<sub>2</sub> loading values on Hg<sup>0</sup> removal were examined using 2, 6, 10, and 15 wt % CeO<sub>2</sub>, respectively, at 150 °C, and the experimental results are shown in Figure 3. ACF impregnation with CeO<sub>2</sub>, particularly when the loading value was 6%, increased the Hg<sup>0</sup> removal amount significantly. When the chemical loading value changed from 0 to 6%, the Hg<sup>0</sup> removal efficiency increased from an average of 60 to 90%. However, the Hg<sup>0</sup> removal ability of ameliorated ACF was not enhanced consistently and decreased when the CeO<sub>2</sub> load increased above 6%. Especially with a loading value of 15%, the Hg<sup>0</sup> removal efficiency declined to 70%.

In comparison to ACF, the samples impregnated with CeO<sub>2</sub> show stronger Hg<sup>0</sup> removal capability, which may be due to the following reasons: first, although many functional groups, such as lactonic, carboxyl, carbonyl, and phenol

**Figure 3.** Effect of the loading value of ACF on the Hg<sup>0</sup> removal efficiency at 150 °C.**Figure 4.** FTIR analysis of ACF and 10% CeO<sub>2</sub>/ACF.

groups are present in the surface of ACF, only lactonic and carbonyl groups play an important role in the Hg<sup>0</sup> removal process.<sup>25</sup> It can be seen from Figure 4 that there are certain differences among the wavenumber bands of ACF and 10% CeO<sub>2</sub>/ACF, and bands at 1400–1680 cm<sup>-1</sup>, which are characteristic absorption peaks of lactonic and carbonyl groups, have been detected in Figure 4.<sup>26</sup> Therefore, the ceria deposition process can produce an additional oxidation of the carbon surface and form more lactonic and carbonyl groups.<sup>27</sup> Second, CeO<sub>2</sub> can act as an oxygen reservoir by storing or releasing O via the Ce<sup>4+</sup>/Ce<sup>3+</sup> redox couple; hence, it has a very important catalysis in a large number of important reactions.<sup>28</sup> In this experiment, it can catalytically enhance the reaction of Hg<sup>0</sup> and O<sub>2</sub> or the sample surface active groups, as shown in the following reactions:

(26) Qi, G.; Yang, R. T.; Chang, R. *Appl. Catal., B* **2004**, *51*, 93.(27) Serrano-Ruiz, J. C.; Ramos-Fernandez, E. V.; Silvestre-Albero, J.; Sepulveda-Escribano, A.; Rodriguez-Reinoso, F. *Mater. Res. Bull.* **2008**, *43*, 1850–1857.(28) Kilgroe, J.; Fornasiero, P.; Graziani, M. *Catal. Today* **1999**, *50*, 285–298.

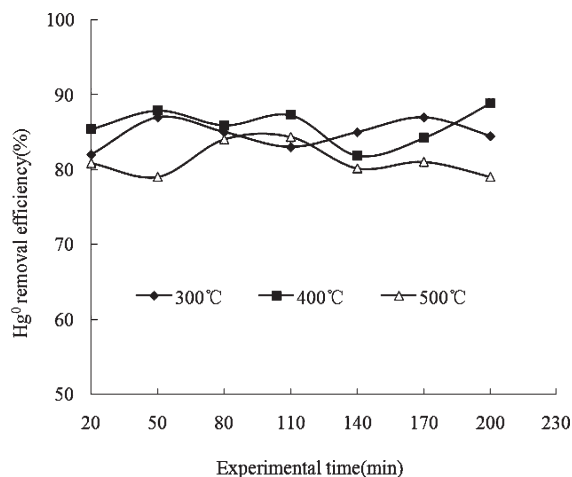


**Figure 5.** Effect of the calcination temperature of the samples.

Third, the key point conditioning the enhanced catalytic properties of samples is the degree of ceria dispersion, and a high degree of ceria dispersion can be seen from Figure 2b.<sup>28–30</sup> On the basis of Table 1 and Figure 3, it is found that ACF with the largest surface area had the minimum  $\text{Hg}^0$  removal performance. When the loading value rose above 6%, the  $\text{Hg}^0$  removal efficiency decreased with the increase in  $\text{CeO}_2$  loading. In the  $\text{Hg}^0$  removal reaction of 6%  $\text{CeO}_2/\text{ACF}$ , at the beginning,  $\text{Hg}^0$  was adsorbed onto the surface of ACF by physisorption contributed by van de Waals forces between the  $\text{Hg}^0$  and ACF and then oxidized by the active sites of ACF surfaces.<sup>9</sup> The increase of the loading value contributed to the decrease of the BET surface area of ACF, which affected the physisorption. When the loading value exceeded a critical point, the  $\text{Hg}^0$  removal efficiency of ACF weakened because of both physisorption and chemisorption.

### 3.3. Effect of the Calcination Temperature of the Samples.

Samples of 6%  $\text{CeO}_2/\text{ACF}$  calcined at 300, 400, and 500 °C were tested at 150 °C to estimate the influence of the calcination temperatures on the  $\text{Hg}^0$  removal ability, and the results are shown in Figure 5. From the figure, the effects of  $\text{CeO}_2/\text{ACF}$  at the three calcination temperatures on  $\text{Hg}^0$  removal showed a similar performance, with an average mercury removal of approximately 80% in 230 min. These results illustrate that the calcinations at 300 °C for 3 h in a  $\text{N}_2$  atmosphere seemed to be enough to produce the total decomposition of cerium nitrate supported on activated carbon fiber; meanwhile, the calcination did not destroy the textural properties of ACF at 300, 400, and 500 °C.

**3.4. Temperature Effect.** Further investigation on the  $\text{Hg}^0$  removal efficiency by 6%  $\text{CeO}_2/\text{ACF}$  was carried out to observe the change of performance over a wide range of temperatures (90–210 °C), and experimental results are shown in Figure 6. From the curves, we can find that 6%  $\text{CeO}_2/\text{ACF}$  shows low  $\text{Hg}^0$  removal ability at 90 °C, approximately 50%. As the reaction temperature increased, the amount of  $\text{Hg}^0$  removal improved progressively and reached the maximum at 150 °C, about 90%. Nonetheless, with the continuous increase of the temperature, the trend was entirely different. For example, when the temperature rose

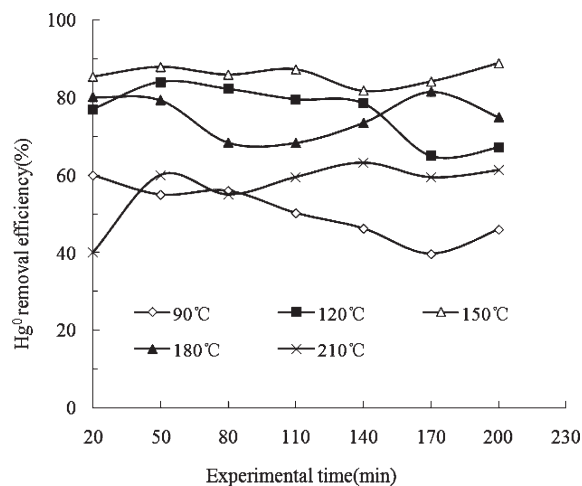


**Figure 6.** Effect of the reaction temperature on the  $\text{Hg}^0$  removal efficiency by 6%  $\text{CeO}_2/\text{ACF}$ .

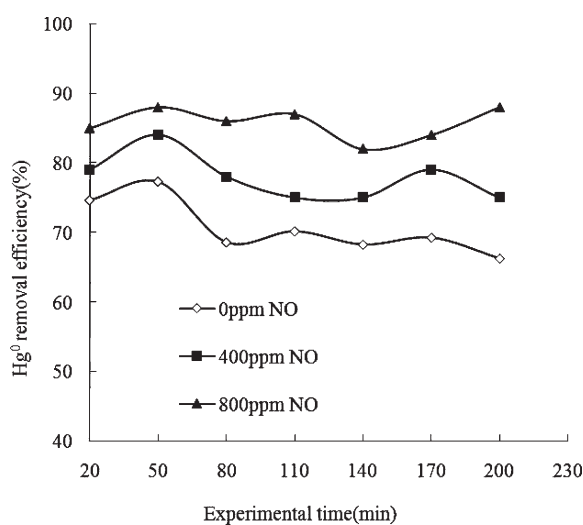


**Figure 7.** Effect of NO on the  $\text{Hg}^0$  removal by 6%  $\text{CeO}_2/\text{ACF}$  at 150 °C.

from 150 to 210 °C, the  $\text{Hg}^0$  removal efficiency decreased from an average of 90 to 60%.

The chemical reaction is more sensitive to the reaction temperature. As the experimental temperature rises, reactants can obtain more kinetic energy, which enhances the catalytic activity of the samples for the oxidation of  $\text{Hg}^0$ .<sup>22</sup> In this experiment, the  $\text{Hg}^0$  removal efficiency was progressively promoted while the temperature increased. However, when the temperature exceeded 150 °C, the  $\text{Hg}^0$  removal ability decreased. Those results manifested that the amount of  $\text{Hg}^0$  removal by  $\text{CeO}_2/\text{ACF}$  could be attributed to a combined chemisorption and physisorption. However, adsorbed  $\text{Hg}^0$  could drop again with the increase of the temperature because of the exothermic nature of the adsorption processes.<sup>30</sup>

**3.5. Effect of NO.** To investigate the effect of NO on the  $\text{Hg}^0$  removal ability, the experiments were carried out with different concentrations of NO (0, 400, and 800 ppm) in experimental gas by using 6%  $\text{CeO}_2/\text{ACF}$  at 150 °C. The experimental results are shown in Figure 7. When there was NO in the experimental gas, the  $\text{Hg}^0$  removal ability of  $\text{CeO}_2/\text{ACF}$  increased from 70 to 90%. This phenomenon can be ascribed to the following mechanism. First, NO

(29) Hu, C. X.; Zhou, J. S.; He, S.; Luo, Z. Y.; Cen, K. F. *Fuel Process. Technol.* **2009**, *90*, 812–817.

(30) Tian, L. H.; Li, C. T.; Li, Q.; Zeng, G. M.; Gao, Z.; Li, S. H. *Fuel* **2009**, *88*, 1687–1691.

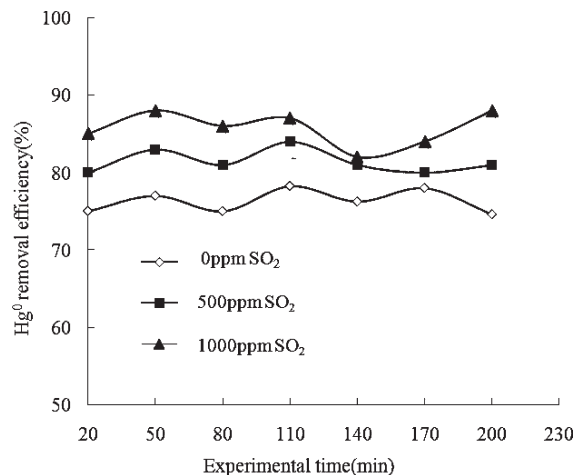
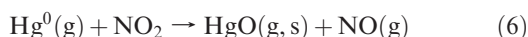
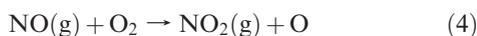


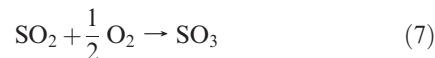
**Figure 8.** Effect of SO<sub>2</sub> on the Hg<sup>0</sup> removal by 6% CeO<sub>2</sub>/ACF at 150 °C.

could react with O<sub>2</sub> to form NO<sub>2</sub> and active O atoms, and then Hg vapor could react with active O atoms and NO<sub>2</sub> to produce HgO.<sup>31–35</sup>



**3.6. Effect of SO<sub>2</sub>.** Figure 8 shows the effects of SO<sub>2</sub> on the Hg<sup>0</sup> removal ability of 6% CeO<sub>2</sub>/ACF at 150 °C in the presence of 0–1000 ppm SO<sub>2</sub> to reveal the efficiency of Hg<sup>0</sup> removal increasing up to 90% from an initial level of 75%, manifesting that SO<sub>2</sub> had a promotional effect on Hg<sup>0</sup> removal. Both Hg<sup>0</sup> and SO<sub>2</sub> could be adsorbed by ACF, but

the competition of the two for similar active sites on the ACF surface is minimized.<sup>36,37</sup> In an oxidizing atmosphere, SO<sub>2</sub> was catalyzed by CeO<sub>2</sub> to form SO<sub>3</sub>, which constituted new chemisorption sites for Hg<sup>0</sup> by reacting with Hg<sup>0</sup> to produce HgSO<sub>4</sub>.<sup>33,38</sup> The mechanism was proposed as follows:



#### 4. Conclusions

In the present paper, the Hg<sup>0</sup> removal ability was studied in a lab-scale fixed-bed system. It is found that the ceria deposition process produces many functional groups from which the Hg<sup>0</sup> removal benefits. However, the specific surface area of CeO<sub>2</sub>/ACF decreases with the increase in the loading value of CeO<sub>2</sub>, which is not conducive to adsorption of Hg<sup>0</sup>. Therefore, in mercury removal by CeO<sub>2</sub>/ACF, it is well-known that physisorption and oxidation are effective. The decomposition of the cerium nitrate precursor is achieved at about 300 °C. From the temperature effect tests, we can find that high temperature improved the oxidation capability of Hg<sup>0</sup> but undermined the adsorption of ACF. Both NO and SO<sub>2</sub> can enhanced Hg<sup>0</sup> oxidation in the experimental gases with an O<sub>2</sub> atmosphere.

The results obtained from this research show that CeO<sub>2</sub>/ACF has great application potential on the Hg<sup>0</sup> removal from flue gas because of higher mercury removal efficiency and longer tolerance time. In addition, it has been proven that CeO<sub>2</sub>/ACF is effective for selective catalytic reduction (SCR) of NO; therefore, it is feasible to remove efficiently Hg<sup>0</sup> and NO<sub>x</sub> from the flue gas in the existing SCR device.

**Acknowledgment.** The authors gratefully acknowledge the financial support of Project 50878080 of the National Natural Science Foundation of China and the Scientific and Technological Project (2008) GK3118 of the Hunan Province in China.

(31) Wang, Y. J.; Duan, Y. F.; Yang, L. G.; Zhao, C. S.; Shen, X. L.; Zhang, M. Y. *Fuel Process. Technol.* **2009**, *90*, 643–651.

(32) Wang, Z. H.; Zhou, J. H.; Zhu, Y. Q.; Wen, Z. C.; Liu, J. Z.; Cen, K. F. *Fuel Process. Technol.* **2007**, *88*, 817–823.

(33) Zhou, J. S.; Luo, Z. Y.; Hu, C. X. *Energy Fuels* **2007**, *21*, 491–495.

(34) Li, Y.; Murphy, P.; Wu, C. Y. *Fuel Process. Technol.* **2008**, *89*, 567–573.

(35) Niksa, S.; Helble, J. J.; Fujiwara, N. *Environ. Sci. Technol.* **2001**, *35*, 3701–3706.

(36) Ochiai, R.; Uddin, M. A.; Sasaoka, E.; Wu, S. J. *Energy Fuels* **2009**, *23*, 4734–4739.

(37) Wang, J. W.; Yang, J. L.; Liu, Z. J. *Fuel Process. Technol.* **2010**, *91*, 676–680.

(38) Eswaran, S.; Stenger, H. G. *Energy Fuels* **2007**, *21*, 852–857.